Structure, Vol. 9, 597–604, July, 2001, ©2001 Elsevier Science Ltd. All rights reserved. PII S0969-2126(01)00619-0

Crystal Structure of the α-Actinin Rod Reveals an Extensive Torsional Twist

Jari Ylänne,[1] Klaus Scheffzek, Paul Young,[3] and Matti Saraste[2]
European Molecular Biology Laboratory, EMBL
Structural and Computational Biology Programme
Meyerhofstrasse 1
D-69117, Heidelberg
Germany

Summary

Background: α-Actinin is a ubiquitously expressed protein found in numerous actin structures. It consists of an N-terminal actin binding domain, a central rod domain, and a C-terminal domain and functions as a homodimer to cross-link actin filaments. The rod domain determines the distance between cross-linked actin filaments and also serves as an interaction site for several cytoskeletal and signaling proteins.

Results: We report here the crystal structure of the α-actinin rod. The structure is a twisted antiparallel dimer that contains a conserved acidic surface.

Conclusions: The novel features revealed by the structure allow prediction of the orientation of parallel and antiparallel cross-linked actin filaments in relation to α-actinin. The conserved acidic surface is a possible interaction site for several cytoplasmic tails of transmembrane proteins involved in the recruitment of α-actinin to the plasma membrane.

Introduction

The actin cytoskeleton is essential for cell movement. In migrating cells, dynamic assembly and disassembly of the actin network drives cell motility, and in muscle, a stable actomyosin filament system forms the contractile apparatus (for reviews see [1, 2]). Many actin binding proteins are necessary for the functioning of the actin cytoskeleton. α-Actinin is a ubiquitous protein that cross-links actin filaments both in muscle and nonmuscle cells [3]. It is found at the leading edge, cell adhesion sites, focal contacts, and along actin stress-fibers in migrating cells [4]. In striated muscle, α-actinin is a major constituent of the Z-disc structure that links adjoining sarcomeres [5]. In *Drosophila melanogaster*, mutations in the α-actinin gene are lethal and disrupt the Z-discs [6, 7].

α-Actinin belongs to a superfamily of actin binding proteins that includes spectrin, dystrophin, and utrophin [8, 9]. These proteins have a characteristic actin binding domain that is composed of two calponin-homology (CH) domains. In addition, they contain multiple spectrin repeats, which are the structural elements that generate their elongated shape and determine the nature of actin cross-links. The functional unit of α-actinin is an antiparallel homodimer in which the amino-terminal CH domains together with the carboxy-terminal calmodulin-homology (CaM) domain form the actin binding heads of the molecule, and the spectrin repeats form the connection between these heads [10] (Figure 1). This linker region is composed of four spectrin repeats, and as it appears to be rather rigid, it is called the rod domain. The rod domain determines the distance between the cross-linked filaments. It also serves as an interaction site for many transmembrane receptors and signaling and adaptor proteins [11–18].

Electron microscopic studies have shown that the actin binding head domains of α-actinin can attain several different conformations through the movements of a flexible neck region between the rod and head [19, 20]. This neck region is also sensitive to proteolytic cleavage [21]. Still, it is not clear how α-actinin cross-links can be found in both antiparallel and parallel actin filaments in vitro and in vivo [22, 23]. This difference in cross-linking topology may require up to a 180° difference in the relative orientation of the actin binding sites. Extending an earlier work on two spectrin repeats of the α-actinin rod [24], we report here the structure of the complete rod domain and discuss its implications for actin cross-linking topology and other protein interactions.

Results

To obtain further insight into the molecular details of F-actin cross-linking structures, such as those in the muscle Z-disc, the full rod domain of human skeletal muscle α-actinin 2A was expressed in *Escherichia coli*, purified, and crystallized. This fragment comprises four spectrin repeats (Figure 1). The structure was determined by molecular replacement using the previously determined crystal structure of repeats 2 and 3 [24] as the search model. The structure was refined at 2.8 Å, resulting in an R_{free} of 29.5% for a model comprising 950 residues (Table 1).

The structure of the α-actinin rod is an antiparallel homodimer with a length of about 240 Å and a diameter of 32–49 Å (Figures 2a and 2b). The major differences between the four spectrin repeats reside in the loop regions (Figure 3b). The loop between helices 2 and 3 seems to be shorter in spectrin repeat 2 than in the others. However, superimposition of the domains and calculation of the rms differences for 70 Cα atoms in the helical sections show that spectrin repeat 1 is the most divergent from the others (Table 2). The same ob-

[1] Correspondence: ylanne@embl-heidelberg.de
[2] Deceased
Present address: [3] Department of Neurobiology, Duke University Medical Center, Durham, North Carolina, USA.

Key words: α-actinin; actin filament; cytoskeleton; crystallography; spectrin repeat

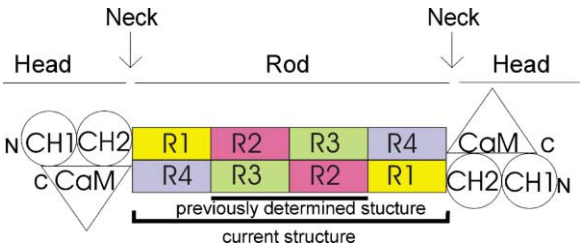

Figure 1. Cartoon of the Domain Structure of α-Actinin

α-Actinin is a homodimer of 200 kDa. The monomer is composed of seven domains: the two N-terminal calponin-homology domains (CH1, CH2) and the C-terminal calmodulin-homology domain (CaM) form the actin binding heads of the molecule, and four spectrin repeats (R1-R4) form the dimeric central rod of the molecule. The fragment studied in this paper and the previously determined structure are indicated.

servation holds when other main chain segments are included in the comparison.

A prominent feature of the overall structure is a left-handed twist from one end of the rod to the other (Figure 2). The twist can be described in the following way: spectrin repeats 1 and 2 of both monomers are parallel to the long axis of the molecule. Spectrin repeats 3 and 4 twist in a left-handed direction over spectrin repeats 1 and 2 of the opposing monomer, forming a 12° angle to the long axis of the molecule. The major tilting occurs between spectrin repeats 2 and 3, and repeats 3 and 4 are again roughly parallel (Figure 2c) This twist leads to a structure in which the terminal faces of the rod are related to each other by an angle of ~90° (Figure 2d).

The twist is associated with a curved dimer interface. We have analyzed this interface in detail to test whether the subunit interaction could be altered and allow differences in the twist. The interface surface extends throughout the molecule and buries 11% (3174 Å^2) of the accessible surface area of a monomer. The interface involves 42% polar and 58% nonpolar atoms, and 12 salt bridges are predicted. This is consistent with the previously observed high affinity of dimer interaction (K_d ≈10 pM) [25, 26]. The net charge on the interface forms a gradient from slightly basic in spectrin repeat 1 to acidic in repeat 4 (Figure 3a). The interfaces between spectrin repeats 1–4 and 2–3 are quite different, involving characteristic contact regions in each of the repeats (Figure 3b). Taken together, these properties suggest that the dimer contact is specific, intimate, and tight. Thus, torsional flexibility of the rod is unlikely, and the twist is a built-in feature of the structure.

To answer the question of whether the twist might be a general feature of different α-actinin isoforms, we have compared the contact residues at the dimer interface of α-actinins from human (*Homo sapiens*), chicken (*Gallus gallus*), fruit fly (*Drosophila melanogaster*), nematode (*Caenohabditis elegans*), and amoeba (*Dictyostelium discoideum*). Generally, the sequences that cover the rod domain are very conserved: the residues in the α-helical regions are 90.4% identical in all the sequences and 88.3% in the nonhelical regions. The dimer contact residues are 92.4% and 91.3% identical in the α-helical and nonhelical regions, respectively. This suggests that the dimer interface, and subsequently the twist in the rod domain, are conserved features of all α-actinins.

The analysis of charge properties and conservation on the surface of the rod domain may help us to gain further insight into potential interaction sites (Figure 4). Overall, the surface of the molecule is relatively acidic; there are no clear basic patches. However, one face of the rod is more acidic than the rest of the surface. Because of the twist, the acidic surface has a concave appearance (Figure 4a). The same surface is also more highly conserved between α-actinin isoforms than the rest of the molecule (Figure 4b). This suggests that the acidic surface of the rod domain is a common feature of all α-actinins and is probably involved in interactions that are vital to their function.

Discussion

The major findings of this paper are, first, that the α-actinin rod is an elongated antiparallel homodimer with

Table 1. Data Statistics

	Dataset 1	Dataset 2
Data Collection		
Space group	$P3_1$	$P3_1$
Unit cell	a = b = 102.7 Å, c = 219.3 Å	a = b = 103.3 Å, c = 218.6 Å
Resolution[a]	3.1 Å (3.2–3.1 Å)	2.8 Å (2.9–2.8 Å)
Number of observations	134,802	155,820
Number of unique reflections	45,996	64,207
I/σ[a]	9.72 (3.26)	7.60 (2.28)
Completeness[a]	98.1% (98.5%)	98.7% (99.0%)
R_{merge}[a]	0.083 (0.283)	0.082 (0.261)
Refinement		
Resolution range	32–3.1 Å	200–2.8 Å
Number of reflections	45,994	70,770
R_{work}	0.282	0.270
R_{free}	0.300	0.295
Rmsd form ideality		
Bonds	0.009 Å	0.008 Å
Angles	1.40°	1.35°

[a] The numbers in parentheses give values for the highest resolution bin.

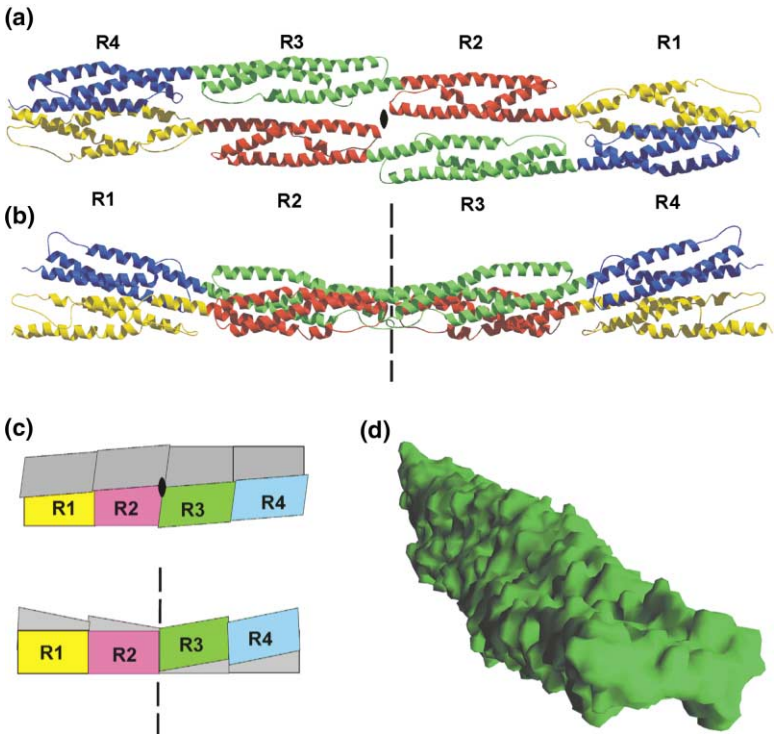

Figure 2. The Overall Structure of the α-Actinin Rod

(a) Ribbon diagrams of the final model along the two-fold symmetry axis of the molecule. Domain coloring is as follows: R1, yellow; R2, red; R3, green; and R4, blue. Note that the vectors from the N and C termini of the opposing monomers are oriented along the two-fold symmetry axis of the molecule.

(b) A view perpendicular to the symmetry axis and to the long axis of the molecule.

(c) A slightly exaggerated diagram indicating the localization of the individual spectrin repeats related to others in the dimer. The major twist is between R3 and R4.

(d) A surface view from the end of the molecule, revealing the ~90° twist between the termini of the molecule.

an extensive and specific interface that spans the length of the molecule. Second, the rod is twisted ~90° from one end to the other, and we predict that the twist is a conserved feature of all α-actinin isoforms. Third, the α-actinin rod has a conserved acidic surface that might have functional importance for molecular recognition. These points and the implications of the structure on the geometry of actin cross-linking are discussed in further detail below.

Dimerization

Using electron microscopy, the α-actinin rod has been found to be a rigid structure that does not bend [19, 20, 22, 27, 28]. The dimensions of the present crystal structure (242 Å × 31–49 Å) are close to those measured from electron microscopic images (250 Å × 40 Å [29]). The rigidity of the rod is apparently generated by the long dimer interface. In line with the previously observed high affinity of dimer formation ($K_d \approx 10$ pM) [25, 26], the crystal structure confirms that the dimer interface is extensive and tight. Ionic interactions have a major role in the dimer formation. Alone, the monomers may be more flexible, but as a dimer, most of the bending and twisting motions would force changes in the interface interactions.

Recently, the structure of spectrin repeats 1 and 2 from the *Dictyostelium discoideum* α-actinin has been determined as an engineered lever arm of myosin [30]. The individual spectrin repeats in our structure superimpose relatively well with the corresponding *Dictyostelium* repeats, but the orientation of the adjacent repeats relative to each other differs (Figure 5). The major differences between the structures are located close to the interface between the spectrin repeats. The linker helix contains no insertions or deletions, but the third helix of spectrin repeat 1 in our structure seems to be disrupted by a glycine that is present in all other α-actinin sequences, except in that of *Dictyostelium*. On the other hand, the *Dictyostelium* structure corresponds to a monomer [30], whereas the structure reported here is the biologically relevant dimer. This may explain the different conformations of the linker helix. Flexibility between individual spectrin repeats has also been noted earlier by comparing the various crystal forms of α-spectrin repeats 16 and 17 [31].

The Twist

A striking feature of the α-actinin rod is the 90° left-handed twist between the ends of the molecule. The twist may have an important structural role in stabilizing the rod and preventing bending motion. On the other hand, the twist restrains the orientation of the actin binding head domains of α-actinin. A twist in the α-actinin molecule has been reported earlier in two-dimensional crystals studied by electron microscopy [19]. In the earlier studies, it has not been possible to distinguish the twist of the rod from alternating orientations of the head. The sequence comparisons suggest that the dimer interface, and thus also the twist of the rod, is a conserved feature of the many α-actinin isoforms.

Implications for Actin Cross-Linking

Electron microscopic studies have shown that the actin binding head domains of α-actinin can adopt several different conformations through the movements of a flexible neck region between the rod and head [19, 20]. Flexibility of the neck region is also suggested by its sensitivity to proteolytic cleavage [21]. Still, it is not clear how α-actinin cross-links are assembled in both antiparallel and parallel actin filament bundles in vitro

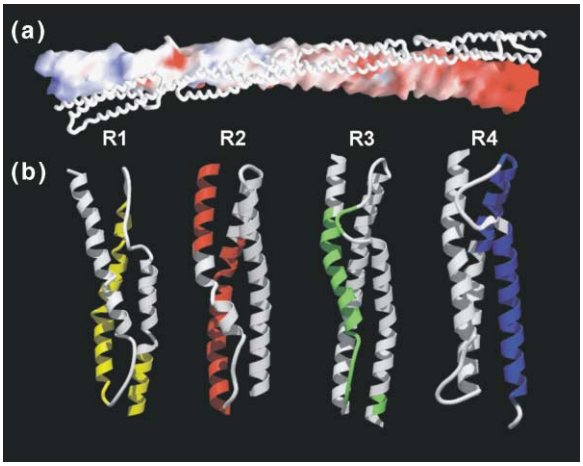

Figure 3. Dimer Interface

(a) Visualization of the dimer interface surface. One monomer is shown as a surface representation and is colored according to surface potential. The other monomer is shown as a backbone worm representation to reveal the location of the interface surface. Surface charge distribution on the interface reveals a gradient from slightly basic (R1 on the left of the surface representation) to acidic (R4 on the right).

(b) The comparison of the areas involved in the dimer interface of the various spectrin repeats. The spectrin repeats are oriented so that the N terminus is on the top left and the C terminus is on the bottom right. The areas of the domains involved in the dimer interface are colored. This representation shows that all four spectrin repeats have the same basic fold, with some modifications, and that each domain has its specific segments involved in the dimer interface .

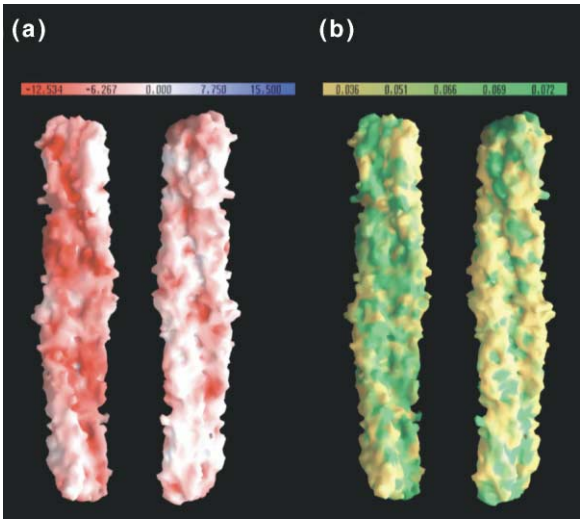

Figure 4. Surface Properties of the Structure

(a) The surface charge potential distribution on the rod molecule. Both views are roughly along the two-fold symmetry axis of the molecule. The concave surface shown on the left is predominantly acidic. The edges of the structure are neutral and partially hydrophobic.

(b) Same views as in (a), showing the surface representation of conserved surface areas between the seven different α-actinin sequences. Green shows the conserved residues, and yellow shows the less conserved residues. The concave surface is predominantly conserved.

and in vivo [22, 23]. The isoforms seem to have different preferences for parallel or antiparallel cross-linking [22]. For instance, the smooth muscle isoform of α-actinin preferentially cross-links antiparallel filaments in solution. The two-dimensional actin bundles that have been studied on lipid monolayers show that skeletal, cardiac, and smooth muscle isoforms of α-actinins can form both bipolar (antiparallel) and polar (parallel) bundles [23, 27]. This difference in cross-linking topology requires a 180° difference in the orientation of the actin binding sites.

Because there apparently is only a single binding mode between an actin filament and α-actinin, the torsional 90° twist of the rod domain cannot explain the various actin filament cross-linking conformations. Furthermore, based on the extensive dimer contacts, we predict that the twist is a stable feature of the rod and is not likely to allow large torsional flexibility. Thus, neck movements are the key feature for the conformational flexibility of α-actinin. Although we do not have any parts of the head domain in our current structure, our data have implications on the orientation of the head region and for movements of the neck. We can draw some conclusions based on the symmetry features of the rod

Table 2. Comparison of the Individual Spectrin Repeats with Each Other

	R1	R2	R3	R4
R1		2.30 Å	2.25 Å	2.50 Å
R2	2.30 Å		1.42 Å	1.43 Å
R3	2.50 Å	1.42 Å		1.37 Å
R4	2.50 Å	1.43 Å	1.37 Å	

Rms distances between C-α atoms of 70 residues in the three α-helical segments of each domain are given.

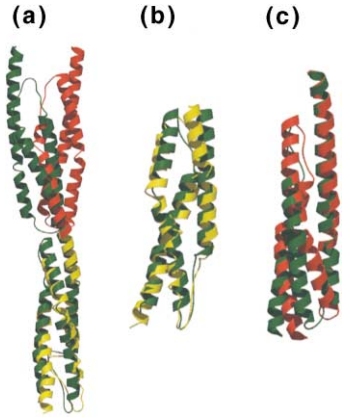

Figure 5. A Comparison between Spectrin Repeats 1 and 2 in Our Structure and *Dictyostelium discoideum* α-Actinin

The color codes are as follows: yellow, human α-actinin 2A repeat 1; red, human repeat 2; and green, *Dictyostelium* α-actinin [30].

(a) Both spectrin repeats cannot be superimposed simultaneously. When the two spectrin repeat 1s are superimposed, the orientations of both spectrin repeat 2s differ.

(b) In the superimposition of the two spectrin repeat 1s, the major differences are the orientations of the helixes linking them to the two spectrin repeat 2s (upper right).

(c) The superimposition of the two spectrin repeat 2s reveals differences at the linking helix (lower left) and the adjoining loop.

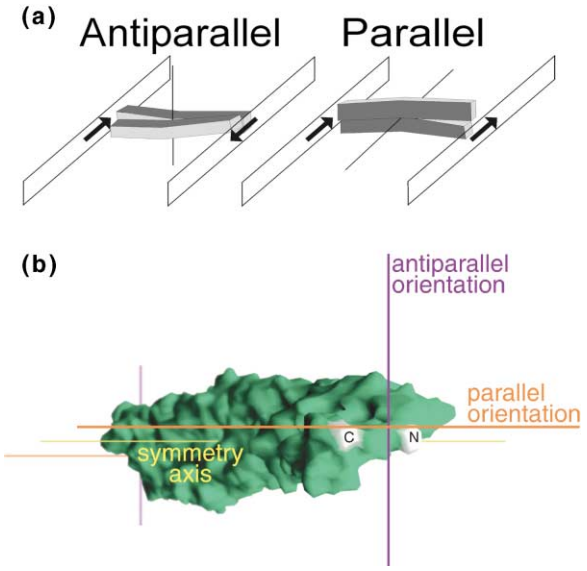

Figure 6. Implications for Actin Filament Cross-Linking Orientation

(a) Predictions of the extreme positions of actin filament orientation based on the symmetry properties of the α-actinin rod domain. If the symmetry properties of the rod extend to the head domains, antiparallel cross-linked actin structures should be oriented perpendicular to the two-fold symmetry axis. Parallel cross-linked actin structures should be oriented along the symmetry axis.

(b) An illustration of the direction of the parallel and antiparallel symmetry element at the end of the rod molecule. The N and C termini are also labeled.

domain and based on the localization of the terminal residues connected to the neck region.

In the current structure, a two-fold symmetry axis perpendicular to the plane of spectrin repeats 1 and 2 penetrates the center of the rod structure. It can be assumed that the parallel and antiparallel cross-linking conformations represent end points of neck movements, and that in these conformations, the ends are symmetric and related by the two-fold axis at the center of the molecule. Thus, the symmetry of the rod might be expanded to the symmetry of the complex between the actin filaments and the cross-linking α-actinin. In such a case, antiparallel cross-linked actin filaments would be perpendicular to this symmetry axis of the rod. Parallel actin filaments should align with the symmetry axis (Figure 6). It has been noticed that α-actinin cross-links preferentially to form an angle of ~60° with the direction of actin filaments, and this seems to apply to both parallel and antiparallel cross-linking conditions [23, 27, 32]. In the antiparallel case, this is compatible with our symmetry considerations. It is more difficult to explain the divergence between the observed orientation of α-actinin cross-links between parallel filaments and our prediction based on the symmetry considerations alone.

In addition to the general consideration related to the symmetry of the molecule, the current structure of the rod gives other hints for the movements of the neck region. The twist and the coiled-coil nature of the spectrin repeats bring the termini of the monomers in such a position that the vectors connecting the N and C termini of the opposing monomers are oriented along the two-fold symmetry axis and are parallel (Figures 2a and 2b). This may determine the hinge axis for neck movement. There are some structural differences between the actin binding domains from proteins homologous to α-actinin [33–35] and also in the interpretation of the electron microscopy data from actin filaments decorated with the actin binding domains [36, 37]. Therefore, we may not yet be in the position of constructing complete atomic models of α-actinin cross-linked actin filaments. Additional experimental data from crystallographic and electron microscopic studies will be needed for such a reconstruction. The current structure and predictions based on its symmetry properties will form an important basis for the future work.

The Conserved Acidic Surface

The concave face of the α-actinin rod seems to be predominantly acidic and well conserved between different isoforms and species. This suggests that this would be a common interaction surface for most, if not all, α-actinin isoforms.

The localization of α-actinin to the plasma membrane is mediated by interactions with phospholipids and with cytoplasmic tails of transmembrane receptors. The sequences of the tail peptides that have been reported to interact with the α-actinin rod are predominantly basic, and many of them have a high α-helical propensity (Table 3). On the basis of the current structure, we predict that these peptides may interact with the conserved acidic surface of the α-actinin rod. The two-fold symmetry of the acidic surface implicates that there are two binding sites for a peptide ligand.

Biological Implications

α-Actinin has at least two major biological functions. It is the major thin filament cross-linking protein in the

Table 3. Transmembrane Receptor Cytoplasmic Domain Peptides Binding to α-Actinin

TM Receptor	α-Actinin Binding Peptide	pI	Length	Reference
NMDA R	RRKQMQL AFAAVNVWRK NLQDRKSGRA EPDP	11.4	31	[50]
ADAM13	RKTLIRLLFT NKKTTIEKLR CVRPSRPPRG	12.0	30	[16]
Integrin β1[a]	FAKFEKEKMNAKW	9.53	13	[11]
Integrin β2	RRFEKEKLKSQ	10.3	11	[40]
ICAM1[a]	RQRKIKYR	11.7	8	[14]
ICAM2[a]	LRQQRMGTYGVRAAWRRLPQAFRP	12.3	24	[15]
L-selectin	RRLKKGKKSKRSMNDPY	11.2	17	[13]
Ep-CAM	RKKRMAK	12.0	7	[51]

[a] The minimal peptide is underlined.

muscle Z-discs, where it holds the adjacent sarcomeres together. On the other hand, α-actinin is found close to the plasma membrane, where it cross-links the cortical actin and serves as a linker between transmembrane receptors and cytoskeleton. The current crystallographic work revealed that the rod domain of α-actinin is torsionally twisted ~90° from one end to another. This is an important piece of information in the attempts to build detailed models of normal and abnormal Z-discs [38]. The analysis of the surface properties of the domain showed a conserved, acidic surface, a possible interaction area for proteins other than actin. One important postulate from the structure is that any protein interacting with the rod domain can potentially have two binding sites on it. Symmetry properties of the structure allowed us to predict the orientation of cross-linked actin filaments in relation to the rod. Thus, in the Z-discs, actin filaments are most probably oriented perpendicular to the two-fold symmetry axis of the α-actinin rod, because this is predicted to be the antiparallel cross-linking orientation of α-actinin. At the cell cortex close to the plasma membrane, the actin filaments should be oriented along the symmetry axis of the α-actinin rod. This is the parallel cross-linking orientation (Figure 6). It is possible that proteins interacting with the α-actinin rod domain are involved in defining the actin cross-linking orientation. At the cell cortex, interactions with cytoplasmic domains of transmembrane receptors that may employ the conserved acidic surface might orient α-actinin such that parallel cross-linking is preferred. These crystallographic results together with biochemical and electron microscopic work will help us and others to build more detailed models of α-actinin cross-links and to understand the role of the signaling molecules that bind to α-actinin in the assembly and maintenance of these structures.

Experimental Procedures

Protein Preparation and Crystallization

A cDNA fragment corresponding to amino acids 274–746 of human skeletal muscle α-actinin (EMBL database M86406) was amplified by a polymerase chain reaction and cloned into a modified [24] pET8c vector (Novagen). The construct contains an NH_2-terminal His_6-tag followed by the cleavage sequence for tobacco etch virus protease ENLYFQGSS [39]. The insert was verified by DNA sequencing. Protein expression was induced in *Esherichia coli* BL21(DE3) at 37°C for 4 hr in the presence of 0.4 mM IPTG. The protein was purified on an Ni-NTA Agarose column (Qiagen), followed by proteolytic removal of the His_6-tag during overnight dialysis against 20 mM Tris (pH 8.0), the second passage through an Ni-NTA column, and ion exchange chromatography on a MonoQ column (Pharmacia). The protein was concentrated to 7–10 mg/ml in 20 mM Tris-HCl, 1 mM DTT (pH 8.0). Crystals were grown at 20°C using hanging-drop vapor diffusion after mixing the protein in a 1:1 volume ratio with the reservoir solution of 0.6–0.8 M NaK-tartrate, 0.1 M HEPES (pH 7.5) (dataset 1) or with 0.9 M $(NH_4)_2SO_4$, 0.1 M Tris-HCL (pH 8.5) (dataset 2). In both conditions, crystals grew overnight and were hexagonal bipyramids with dimensions of up to 0.7 mm in length.

Data Collection and Structure Determination

For dataset 1, crystals were frozen after serial transfer in 5%, 10%, 15%, and 20% ethyleneglycol, 0.9 M NaK-tartrate, 0.1 M HEPES (pH 7.5). Data were collected from a single crystal with a MAR345 image plate detector (X-ray Research GmbH) at the BM-30 beamline in the European Synchrotron Radiation Facility (ESRF) and merged with low-resolution data obtained on a GX-21 rotating anode generator (Elliot-Marconi Avionics) using a similar image plate detector. For dataset 2, crystals were soaked for 5 hr at 23 C° in the presence of 0.5 mM peptide from the cytoplasmic domain of integrin β_2 subunit (KALIHLSDLREYRRFEKEKLKS) [40] in 1 M $(NH_4)_2SO_4$, 0.1 M Tris-HCL (pH 8.5) and frozen after serial transfer in 5%, 10%, 15%, and 20% ethyleneglycol in the same buffer. The dataset was collected from a single crystal at the ID14–2 beamline in ESRF. All data processing and scaling was done with XDS [41].

Molecular replacement calculations for dataset 1 using the coordinates of the dimeric fragment of spectrin repeats 2 and 3 from the same molecule (PDB code 1QUU) [24] (see Figure 1) were performed with AMORE [42] or CNS [43]. The best molecular replacement solution calculated for the data from 10 Å–3.5 Å with this search model covering one half of the complete rod domain gave an R factor of 49%. The electron density map that was generated based on this solution allowed the identification of the α-helical backbones of spectrin repeats 1 and 4 that were missing from the search model. Several cycles of model building using O [44] and refinement with CNS were then performed. Dataset 1 yielded to a partial model of 904 residues (282–348, 360–744) at 3.1 Å resolution. This model was further extended and refined to 2.8 Å by using dataset 2. The crystals of dataset 2 belonged to the same space group and had approximately the same unit cell parameters as dataset 1, although the crystallization conditions were different. No electron density was found for the peptide that was introduced to the crystal for dataset 2.

Consistent with an exceptionally high solvent content of 80%, large solvent-filled cavities were observed covering the regions perpendicular to the c-axis of the unit cell. The elongated molecules pack mainly along the c-axis. This may allow flexibility perpendicular to the c-axis, reflected in the anisotropic diffraction. The final model has 950 residues (274–746) of α-actinin and 2 amino-terminal serine residues from the vector. Spectrin repeat 1 is the least ordered in the structure. There was one break in the main chain electron density map between residues 360 and 361, and model building at this region was partially aided by the crystal structure of *Dictyostelium discoideum* α-actinin spectrin repeat 1 (PDB code 1G8X) [30]. The Ramachandran plot of the final model has 85.1% of the residues in the most favored regions, 11.5% in allowed regions, 2.7% in generously allowed regions, and 0.7% in disallowed regions. The six residues with the disallowed Ramachandran angles were all located in the loop regions. Structure figures were generated with Molscript [45], Raster3D [46], and GRASP [47]. Sequence alignment was generated with ClustalX [48]. The dimer interaction was analyzed by using the server http://www.biochem.ucl.ac.uk/bsm/PP/server [49]. Superimposition of the domains was performed with O.

Acknowledgments

We thank Drs. Mathias Gautel, Kristina Djinovic, and Michael Way for critical comments and discussion, the ESRF beamline staff for their help, and Drs. J. Kull, W. Kliche, and D. Manstein for kindly providing coordinates of *Dictyostelium* α-actinin spectrin repeats 1 and 2 before release.

Received: February 21, 2001
Revised: May 7, 2001
Accepted: June 5, 2001

References

1. Borisy, G.G., and Svitkina, T.M. (2000). Actin machinery: pushing the envelope. Curr. Opin. Cell Biol. *12*, 104–112.
2. Geeves, M.A., and Holmes, K.C. (1999). Structural mechanism of muscle contraction. Annu. Rev. Biochem. *68*, 687–728.
3. Otto, J.J. (1994). Actin-bundling proteins. Curr. Opin. Cell Biol. *6*, 105–109.
4. Knight, B., Laukaitis, C., Akhtar, N., Hotchin, N.A., Edlund, M., and Rick Horwitz, A. (2000). Visualizing muscle cell migration in situ. Curr. Biol. *10*, 576–585.
5. Masaki, T., Endo, M., and Ebashi, S. (1967). Localization of

6S component of an alpha-actinin at Z-band. J. Biochem. *62*, 630–632.
6. Fyrberg, C., Ketchum, A., Ball, E., and Fyrberg, E. (1998). Characterization of lethal *Drosophila melanogaster* alpha-actinin mutants. Biochem. Genet. *36*, 299–310.
7. Fyrberg, E., Kelly, M., Ball, E., Fyrberg, C., and Reedy, M.C. (1990). Molecular genetics of *Drosophila* alpha-actinin: mutant alleles disrupt Z disc integrity and muscle insertions. J. Cell Biol. *110*, 1999–2011.
8. Hitt, A.L., and Luna, E.J. (1994). Membrane interactions with the actin cytoskeleton. Curr. Opin. Cell Biol. *6*, 120–130.
9. Winder, S.J. (1997). The membrane-cytoskeleton interface: the role of dystrophin and utrophin. J. Muscle Res. Cell Motil. *18*, 617–629.
10. Critchley, D.R. (2000). Focal adhesions - the cytoskeletal connection. Curr. Opin. Cell Biol. *12*, 133–139.
11. Otey, C.A., Pavalko, F.M., and Burridge, K. (1990). An interaction between alpha-actinin and the beta-1 integrin subunit in vitro. J. Cell Biol. *111*, 721–729.
12. Pavalko, F.M., and LaRoche, S.M. (1993). Activation of human neutrophils induces an interaction between the integrin beta 2-subunit (CD18) and the actin binding protein alpha-actinin. J. Immunol. *151*, 3795–3807.
13. Pavalko, F.M., Walker, D.M., Graham, L., Goheen, M., Doerschuk, C.M., and Kansas, G.S. (1995). The cytoplasmic domain of L-selectin interacts with cytoskeletal proteins via alpha-actinin: receptor positioning in microvilli does not require interaction with alpha-actinin. J. Cell Biol. *129*, 1155–1164.
14. Carpen, O., Pallai, P., Staunton, D.E., and Springer, T.A. (1992). Association of intercellular adhesion molecule-1 (ICAM-1) with actin-containing cytoskeleton and alpha-actinin. J. Cell Biol. *118*, 1223–1234.
15. Heiska, L., et al., and Carpen, O. (1996). Binding of the cytoplasmic domain of intercellular adhesion molecule-2 (ICAM-2) to alpha-actinin. J. Biol. Chem. *271*, 26214–26219.
16. Galliano, M.F., Huet, C., Frygelius, J., Polgren, A., Wewer, U.M., and Engvall, E. (2000). Binding of ADAM12, a marker of skeletal muscle regeneration, to the muscle-specific actin-binding protein, alpha-actinin-2, is required for myoblast fusion. J. Biol. Chem. *275*, 13933–13939.
17. Papa, I., et al., and Benyamin, Y. (1999). Alpha actinin-CapZ, an anchoring complex for thin filaments in Z-line. J. Muscle Res. Cell Motil. *20*, 187–197.
18. Chien, K.R. (2000). Genomic circuits and the integrative biology of cardiac diseases. Nature *407*, 227–232.
19. Taylor, K.A., and Taylor, D.W. (1993). Projection image of smooth muscle alpha-actinin from two-dimensional crystals formed on positively charged lipid layers. J. Mol. Biol. *230*, 196–205.
20. Winkler, J., Lunsdorf, H., and Jockusch, B.M. (1997). Flexibility and fine structure of smooth-muscle alpha-actinin. Eur. J. Biochem. *248*, 193–199.
21. Mimura, N., and Asano, A. (1986). Isolation and characterization of a conserved actin-binding domain from rat hepatic actinogelin, rat skeletal muscle and chicken gizzard alpha-actinins. J. Biol. Chem. *261*, 10680–10687.
22. Meyer, R.K., and Aebi, U. (1990). Bundling of actin filaments by alpha-actinin depends on its molecular length. J. Cell Biol. *110*, 2013–2024.
23. Taylor, K.A., Taylor, D.W., and Schachat, F. (2000). Isoforms of alpha-actinin from cardiac, smooth, and skeletal muscle form polar arrays of actin filaments. J. Cell Biol. *149*, 635–646.
24. Djinovic-Carugo, K., Young, P., Gautel, M., and Saraste, M. (1999). Structure of the alpha-actinin rod: molecular basis for cross-linking of actin filaments. Cell *98*, 537–546.
25. Flood, G., Kahana, E., Gilmore, A.P., Rowe, A.J., Gratzer, W.B., and Critchley, D.R. (1995). Association of structural repeats in the alpha-actinin rod domain. Alignment of inter-subunit interactions. J. Mol. Biol. *252*, 227–234.
26. Flood, G., Rowe, A.J., Critchley, D.R., and Gratzer, W.B. (1997). Further analysis of the role of spectrin repeat motifs in alpha-actinin dimer formation. Eur. Biophys. J. *25*, 431–435.
27. Taylor, K.A., and Taylor, D.W. (1994). Formation of two-dimensional complexes of F-actin and crosslinking proteins on lipid monolayers: demonstration of unipolar alpha-actinin-F-actin crosslinking. Biophys. J. *67*, 1976–1983.
28. Winkler, J., Lunsdorf, H., and Jockusch, B.M. (1997). Flexibility and fine structure of smooth-muscle alpha-actinin. Eur. J. Biochem. *248*, 193–199.
29. Imamura, M., Endo, T., Kuroda, M., Tanaka, T., and Masaki, T. (1988). Substructure and higher structure of chicken smooth muscle alpha-actinin molecule. J. Biol. Chem *263*, 7800–7805.
30. Kliche, W., Fujita-Becker, S., Kollmar, M., Manstein, D.J., and Kull, F.J. (2001). Structure of a genetically engineered molecular motor. EMBO J. *20*, 40–46.
31. Grum, V.L., Li, D., MacDonald, R.I., and Mondragon, A. (1999). Structures of two repeats of spectrin suggest models of flexibility. Cell *98*, 523–535.
32. Taylor, K.A., and Taylor, D.W. (1999). Structural studies of cytoskeletal protein arrays formed on lipid monolayers. J. Struct. Biol. *128*, 75–81.
33. Goldsmith, S.C., Pokala, N., Shen, W., Fedorov, A.A., Matsudaira, P., and Almo, S.C. (1997). The structure of an actin-crosslinking domain from human fimbrin. Nat. Struct. Biol. *4*, 708–712.
34. Keep, N.H., Norwood, F.L., Moores, C.A., Winder, S.J., and Kendrick-Jones, J. (1999). The 2.0 Å structure of the second calponin homology domain from the actin-binding region of the dystrophin homologue utrophin. J. Mol. Biol. *285*, 1257–1264.
35. Norwood, F.M.L., Sutherland-Smith, A.J., Keep, N.H., and Kendrick-Jones, J. (2000). The structure of the N-terminal actin-binding domain of human dystrophin and how mutations in this domain may cause Duchenne or Becker muscular dystrophy. Structure *8*, 481–491.
36. Hanein, D., et al., and Matsudaira, P. (1998). An atomic model of fimbrin binding to F-actin and its implications for filament crosslinking and regulation. Nat. Struct. Biol. *5*, 787–792.
37. Moores, C.A., Keep, N.H., and Kendrick-Jones, J. (2000). Structure of the utrophin actin-binding domain bound to F-actin reveals binding by an induced fit mechanism. J. Mol. Biol. *297*, 465–480.
38. Luther, P.K. (2000). Three-dimensional structure of a vertebrate muscle Z-band: implications for titin and alpha-actinin binding. J. Struct. Biol. *129*, 1–16.
39. Parks, T.D., Leuther, K.K., Howard, E.D., Johnston, S.A., and Dougherty, W.G. (1994). Release of proteins and peptides from fusion proteins using a recombinant plant virus proteinase. Anal. Biochem. *216*, 413–417.
40. Sampath, R., Gallagher, P.J., and Pavalko, F.M. (1998). Cytoskeletal interactions with the leukocyte integrin beta2 cytoplasmic tail. Activation-dependent regulation of associations with talin and alpha-actinin. J. Biol. Chem. *273*, 33588–33594.
41. Kabsch, W. (1993). Automatic processing of rotation diffraction data from crystals of initially unknown symmetry and cell constants. J. Appl. Crystallogr. *26*, 795–800.
42. CCP4 (1994). The CCP4 (Collaborative Computational Project Number 4) suite: programs for protein crystallography. Acta Crystallogr. D *50*, 760–763.
43. Brunger, A.T., et al., and Warren, G.L. (1998). Crystallography & NMR system: a new software suite for macromolecular structure determination. Acta Crystallogr. D *54*, 905–921.
44. Jones, T.A., Zou, J.Y., Cowan, S.W., and Kjeldgaard (1991). Improved methods for binding protein models in electron density maps and the location of errors in these models. Acta Crystallogr. A *47*, 110–119.
45. Kraulis, P.J. (1991). MOLSCRIPT: a program to produce both detailed and schematic plots of protein structures. J. Appl. Crystallogr. *24*, 946–950.
46. Merritt, E.A., and Murphy, M.E.P. (1994). Raster3D version 2.0. A program for photorealistic molecular graphics. Acta Crystallogr. D *50*, 869–873.
47. Nicholls, A., Sharp, K.A., and Honig, B. (1991). Protein folding and association: insights from the interfacial and thermodynamic properties of hydrocarbons. Proteins *11*, 281–296.
48. Jeanmougin, F., Thompson, J.D., Gouy, M., Higgins, D.G., and Gibson, T.J. (1998). Multiple sequence alignment with Clustal X. Trends Biochem. Sci. *23*, 403–405.

49. Jones, S., and Thornton, J.M. (1996). Principles of protein-protein interactions. Proc. Natl. Acad. Sci. USA *93*, 13–20.
50. Wyszynski, M., et al., and Sheng, M. (1997). Competitive binding of alpha-actinin and calmodulin to the NMDA receptor. Nature *385*, 439–442.
51. Balzar, M., Bakker, H.A., Briaire-de-Bruijn, I.H., Fleuren, G.J., Warnaar, S.O., and Litvinov, S.V. (1998). Cytoplasmic tail regulates the intercellular adhesion function of the epithelial cell adhesion molecule. Mol. Cell. Biol. *18*, 4833–4843.

Accession Numbers

The atomic coordinates of the model have been deposited in the Protein Data Bank under accession number 1hci.